Iranian Society of Acoustics and Vibration
The 15th ISAV2025 International Conference on Acoustics and Vibration
24-25 Dec 2025 Tehran- Iran

Investigation of the Effect of Chaotic Dynamics in Polyurethane Seat Cushion on Ride Comfort of Bell 214 Helicopter Pilots

S.M. Kamali[a*], A. Nouri[b], H.M. Khanlo[c], H. Sabouri[d]

[a]*Department of Aerospace Engineering, Shahid Sattari Aeronautical University of Science and Technology, Tehran, Iran.*

** Corresponding author e-mail: sm.kamali@ssau.ac.ir*

[b]*Department of Aerospace Engineering, Shahid Sattari Aeronautical University of Science and Technology, Tehran, Iran.*

[c]*Department of Aerospace Engineering, Shahid Sattari Aeronautical University of Science and Technology, Tehran, Iran.*

[d]*Faculty of Engineering, Department of Mechanical Engineering, Kharazmi University, Tehran, Iran.*

Abstract.

This study investigates the chaotic dynamics of nonlinear seat cushions and their influence on pilot ride comfort during helicopter operations. Pilot comfort represents a critical aspect of helicopter vibration research; hence, it is necessary to investigate both the seat suspension and the cushion system as the principal contributors to pilot comfort. Among these, the seat cushion holds particular importance due to its cost-effectiveness and significant influence on low-frequency vibration attenuation, which strongly affects perceived comfort. Conventional linear models of polyurethane energy-absorbing cushions are not sufficient to accurately capture their real dynamic behavior. Improper specification of stiffness and damping characteristics can lead to inadequate vibration isolation and, in the long term, potential health risks for pilots. The main innovation of this research lies in systematically evaluating the effect of nonlinear stiffness parameters on the onset of chaotic behavior and assessing their effects on vibration isolation performance. Therefore, the seat cushion is modeled as a mass–spring–damper system, where the nonlinear stiffness coefficient is determined experimentally. Because the cushion model is nonlinear therefore, it has nonlinear dynamic behavior, and this study investigates the relationship between such nonlinear behaviors and ride comfort. The cushion model is incorporated into a 4-DOF biodynamic system and subsequently extended to a 5-DOF model for improved fidelity. The nonlinear dynamic behavior is analyzed through bifurcation diagrams and maximum Lyapunov exponent, and then it is confirmed by other tools such as, time response, phase-plane trajectories, Poincaré maps, and FFT spectra. Next, in the periodic, multi-periodic, and chaotic ranges, the pilot comfort parameters, including transmissibility and mechanical impedance and apparent mass, have been investigated, and the optimal ride comfort ranges have been identified. The results showed that the stiffness properties of the cushion, which cause the dynamic behaviors to be in the chaotic range, significantly increase the seat-to-head transmissibility and increase the mechanical impedance, indicating that the cushion no longer absorbs vibrations but instead amplifies irregular forces. These findings emphasize the importance

of selecting nonlinear properties in the periodic range to ensure stability, achieve effective vibration isolation, and maintain pilot safety and operational comfort during Bell 214 helicopter missions.

Keywords: Ride comfort, Nonlinear, Helicopter, Chaotic behavior, Polyurethane cushion.

1. Introduction

Helicopters, as versatile and essential air vehicles, are subject to dynamic forces that produce unique vibration characteristics that are significantly different from ground transportation forces. These vibrations are primarily caused by the complex dynamics of the rotor and the aerodynamic interactions between the helicopter structure and the surrounding air. The excitation frequencies in helicopters are usually an integer multiple of the rotor speed, which is transmitted to the seat through the airframe and is felt directly by the pilot in his seat. These vibrations, which are sometimes of low frequency and in the range of 0 to 20 Hz, disturb the pilot's comfort and can lead to health consequences such as chronic fatigue, muscle disorders and spinal cord injuries over long periods [1-5].

Dynamic modeling of human–seat interactions under vibration is essential for assessing occupant comfort. Therefore, researchers have developed various biodynamic models, ranging from simple single-degree-of-freedom systems to complex multi-degree-of-freedom systems, to effectively analyze the behavior of the seated body under vibration [6–11].Won & Schimmels 4-DOF analytical model has shown superior performance compared to other multi-DOF models in predicting biodynamic responses, due to its close agreement with experimental data [12]. Biomechanical studies indicate that the upper part of the human body accounts for approximately 73% of the total body mass, with the remainder located in the lower limbs [13].Vertical biodynamic responses and whole-body vibration (WBV) in suspended seats have been reviewed by Boileau and Griffin [14,15].In addition, advanced finite element simulations have been conducted to evaluate improvements in ride comfort under dynamic conditions [16]. Atindana and colleagues proposed a pneumatic seat optimized using the Grey Wolf algorithm to mitigate low-frequency vibrations [17]. Other studies have also highlighted the need for optimized seat cushions in high-vibration environments, such as helicopter pilot seats [18–20].

Much research has focused on seat suspension systems to reduce vibration, while comparatively less attention has been given to the nonlinear properties of seat cushions such as nonlinear damping and stiffness that play a key role in enhancing comfort. Seat cushions in helicopters and airplanes are typically made of polyurethane foam, viscoelastic foam, or composite materials. They function as spring–damper systems exhibiting nonlinear dynamic behavior that depends on load, displacement, and excitation frequency. Polyurethane-based seat cushions are widely used due to their excellent energy absorption capacity, low weight, and effective comfort under dynamic loading conditions [21–23]. Nonlinear dynamics are also observed in automotive suspension systems, aerospace landing gears, and polymer-based vibration isolators. Nonlinear systems, particularly complex vibrating systems, are often prone to chaotic behavior, and understanding such dynamics is essential for predicting system responses and ensuring stability in engineering applications. Among studies that have explored chaotic behavior in mechanical systems [24–26], Zhao investigated the dynamic characteristics of a seat system with nonlinear suspension considering friction effects, showing that incorporating nonlinear and frictional behaviors leads to more accurate predictions of seat vibration responses [27]. Magri et al. presented a comprehensive computational method for evaluating nonlinear elastokinematic properties of passenger car suspension systems, highlighting techniques relevant to modeling complex nonlinear behaviors [28]. Similarly, Chunyan et al. conducted a multifactor analysis of static and dynamic characteristics of membrane air springs in small passenger cars, emphasizing how nonlinear elastic components affect

system performance under varying load conditions [29]. Zhao et al. further analyzed a nonlinear vehicle suspension system under stochastic uncertainties, showing that variability in system parameters significantly affects dynamic responses and ride comfort [30].

Previous studies have advanced our understanding of seat cushions, but have often overlooked the nonlinear properties of materials such as polyurethane and the need for integrated modeling. This study addresses these gaps by experimentally characterizing the nonlinear stiffness of polyurethane cushions and analyzing their effects on vibration transmission and pilot biomechanics using a validated biodynamic model.

The remainder of this paper is organized as follows: Section 2 introduces the biodynamic modeling of the seated human body using a validated 4-degree-of-freedom model, including the equations of motion and the relevant mass, stiffness, and damping parameters. Section 3 provides the experimental characterization of the polyurethane seat cushion and details its nonlinear stiffness properties. Section 4 presents a numerical investigation using a 5-DOF mass-spring-damper model incorporating the measured cushion parameters and analyzes the effects of nonlinear stiffness on the dynamic response of the seated pilot. The transition from periodic to multi-periodic and chaotic behaviors is investigated and their impact on ride comfort is discussed. Finally, the study combines the results to provide insights into the optimal design of the seat cushion to enhance pilot comfort and reduce vibration.

2. Biodynamic mathematical modeling

As previously mentioned, several multi-degree-of-freedom models have been developed to study the dynamic response of the human body to vibrations. Among these, the 4-DOF model proposed by Wan & Schimmels shows a strong correlation with the experimental results reported by Boileau [12], which are considered some of the most reliable experimental data in this field. Additionally, in this study, only vertical vibrations affecting the occupant are considered, as they are the primary factor influencing the pilot's body motion during flight.

Figure 1 illustrates a 4-DOF biomechanical model of the human body. In this model, various body segments are depicted as lumped masses connected by linear springs and dampers. To validate the accuracy of the analytical formulation utilized in this study, the biodynamic equations of motion were reconstructed using the structure and parameters from prior research [12]. Subsequently, the transmissibility parameter, a crucial indicator of ride comfort, was calculated and verified.

In this model, m_1 represents the mass of the head, m_2 the mass of the upper torso, m_3 the mass of the smaller lateral body parts, and m_4 the combined mass of the seat and thighs. The coefficients C_i and K_i represent damping and stiffness parameters, respectively. The equations of motion for each degree of freedom are generally expressed in Equation 1.

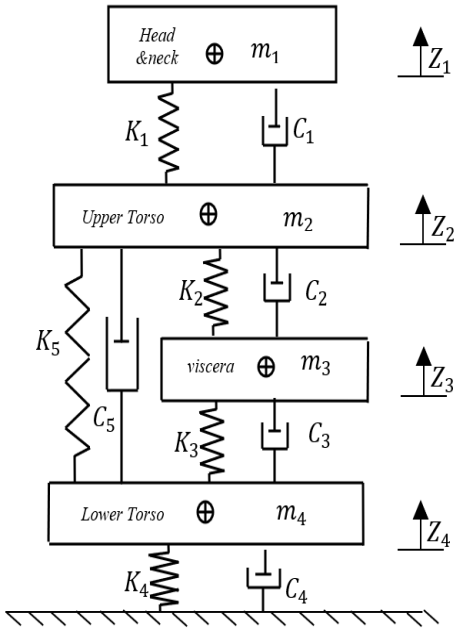

Figure 1. 4-DOF Wan & Schimmels model [12].

$$[M]\ddot{Z}+[C]\dot{Z}+[K]\{Z\}=P \qquad (1)$$

Where the [M], [C], [K], and {P} represent the mass, damping, stiffness matrices, and external excitation forces, respectively. Equations 2 to 5 represent the differential equations of the 4-DOF system of a seated human.

$$m_1\ddot{z}_1+c_1(\dot{z}_1-\dot{z}_2)+k_1(z_1-z_2)=0 \qquad (2)$$

$$m_2\ddot{z}_2+c_1(\dot{z}_2-\dot{z}_1)+k_1(z_2-z_1)+c_2(\dot{z}_2-\dot{z}_3)+k_2(z_2-z_3)+c_5(\dot{z}_2-\dot{z}_4)+k_5(z_2-z_4)=0 \qquad (3)$$

$$m_3\ddot{z}_3+c_2(\dot{z}_3-\dot{z}_2)+k_2(z_3-z_2)+c_3(\dot{z}_3-\dot{z}_4)+k_3(z_3-z_4)=0 \qquad (4)$$

$$m_4\ddot{z}_4+c_5(\dot{z}_4-\dot{z}_2)+k_5(z_4-z_2)+c_3(\dot{z}_4-\dot{z}_3)+k_3(z_4-z_3)+c_4(\dot{z}_4-\dot{z}_0)+k_4(z_4-z_0)=0 \qquad (5)$$

Also $\ddot{z}_i$, $\dot{z}_i$ and z_i represent acceleration, velocity, and displacement values.

To investigate the Bell 214 helicopter ride comfort and effect of vibrations on the pilot's body, the biodynamic equations of motion are usually evaluated by transmissibility, driving point mechanical impedance, and apparent mass. The transmissibility of the seat, mechanical impedance, and apparent mass are introduced in equations 6 to 8.

$$STHT(j\omega)=\frac{X_n(j\omega)}{X_1(j\omega)} \qquad (6)$$

$$DPMI(j\omega)=\frac{F(j\omega)}{V(j\omega)} \qquad (7)$$

$$APMS(j\omega) = \frac{F(j\omega)}{a(j\omega)} \quad (8)$$

Where STHT represents transmissibility, which is the ratio of seat-to-head displacement, DPMI represents driving point mechanical impedance, which is the ratio of excitation force and velocity, and APMS represents the apparent mass, which is the ratio of excitation force and acceleration, jω represents the complex vector of the Fourier transform.

For results verification, as shown in Figure 2, a seated pilot body model, similar to the 4-DOF model of the Wan & Schimmels, with the specifications in Table 1, was analytically modeled in MATLAB software, and the results were examined and compared. Table 1 shows the mass, spring stiffness, and damping characteristics for the 4-DOF Wan & Schimmels model.

Table 1. Characteristics of the mass, stiffness, and damping of the human body [31]

Parameter	Value	Parameter	Value
m_1	6.5(kg)	K_4	173 (kN/m)
m_2	30.5(kg)	K_5	90 (kN/m)
m_3	9.5(kg)	C_1	400 (N.s/m)
m_4	13.5(kg)	C_2	4750 (N.s/m)
K_1	310(kN/m)	C_3	4600 (N.s/m)
K_2	183 (kN/m)	C_4	2600 (N.s/m)
K_3	162 (kN/m)	C_5	2100 (N.s/m)

Figure 2 displays the analytical comparison of the seat-to-head transmissibility parameter in a 4-DOF biodynamic model of a seated occupant with the validated 4-DOF Wan & Schimmels model. It should be noted that this verification step has already been conducted in our previous publication [31], and the consistency of the current results with that study further confirms the robustness of the modeling approach. It is evident that there is a strong agreement between the current analytical model and the Wan & Schimmels model. These results suggest that the modeling steps in the 4-DOF model, as well as the extraction of results, have been executed accurately. Therefore, this type of analysis and modeling can be relied upon for the continuation of this study.

In the following sections, the dynamic properties of the seat cushion are first determined experimentally. Subsequently, numerical analyses are conducted to investigate the nonlinear behavior of the spring and the damping characteristics of the cushion. Finally, the pilot comfort parameters are evaluated and compared across periodic, multi-periodic, and chaotic regions.

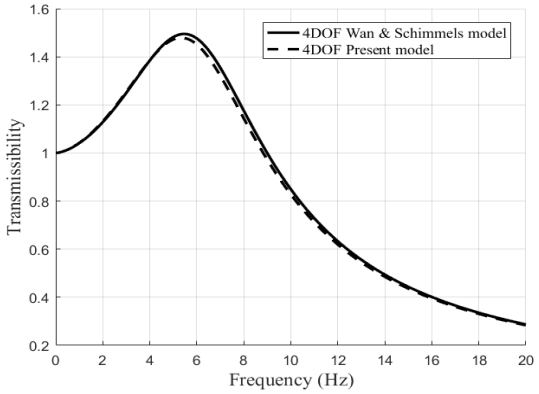

Figure 2. Seat to head transmissibility verification[31]

3. Measurement of seat cushion Dynamic parameters

Choosing the correct materials for Bell 214 helicopter pilot seat cushions is crucial as they need to offer comfort, safety, and durability in challenging operating conditions. Polyurethane foam is a highly effective material for helicopter pilot seat cushions. It absorbs vibrational and impact energy, molds to body contours for ergonomic support, it minimizes vibration transmission to the occupant. Therefore, polyurethane foam was chosen for helicopter pilot seat cushions in this study. Figure 3(a) shows the polyurethane cushion sample utilized in this study.

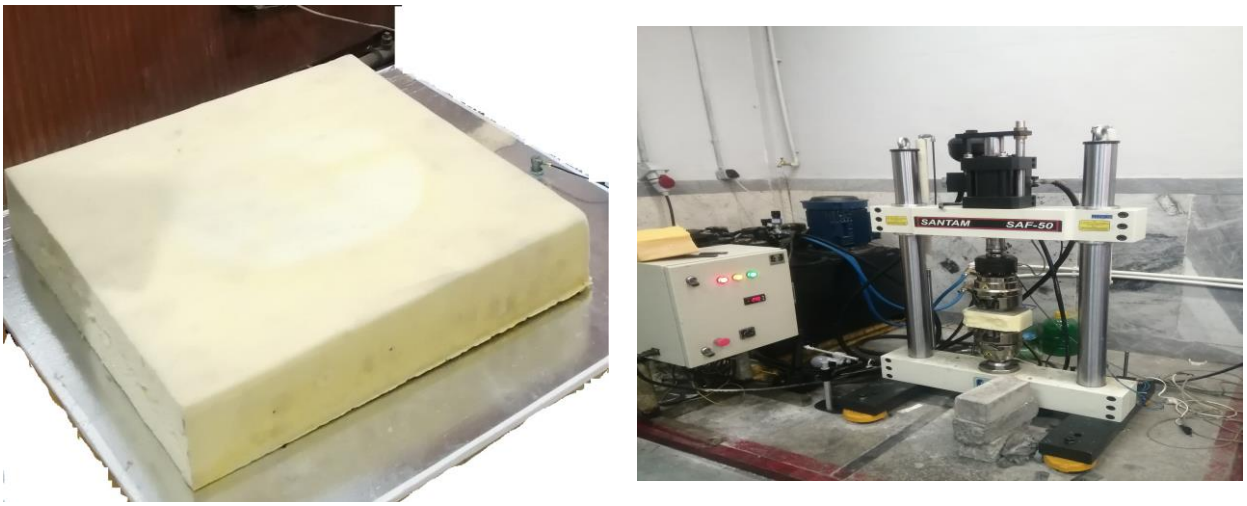

(a) (b)

Figure 3. (a) Polyurethane seat cushion. (b) Experimental measurements of cushion stiffness

The dynamic properties of the polyurethane seat cushion, including stiffness, were initially unknown. To accurately determine these characteristics, experimental testing was conducted using a 5-ton axial fatigue testing machine (SANTAM SAF-50). Figure 3(b) shows a polyurethane specimen with dimensions of 10×10×8 cm, which was subjected to axial loading. The cushion specifications are summarized in Table 2, and its dynamic parameters were determined according to ISO 2439.

Table 2. Characteristics of a polyurethane cushion

Parameter	Value
$\boldsymbol{\rho}$	58 kg/m^3
Porosity	63%
Operating Temperature	$-40℃\ to\ \ 85℃$

To determine the stiffness characteristics of the polyurethane cushion the cushion material was tested under realistic operating conditions, and it was found to exhibit nonlinear behavior. The resulting curve, representing the cushion stiffness recovery cycle, is shown in Figure 4(a). The center line of this cycle represents the nonlinear function of the cushion stiffness coefficient, and the centerline of the cushion force–deflection curve along with its linearized approximation are shown in Figure 4(b).

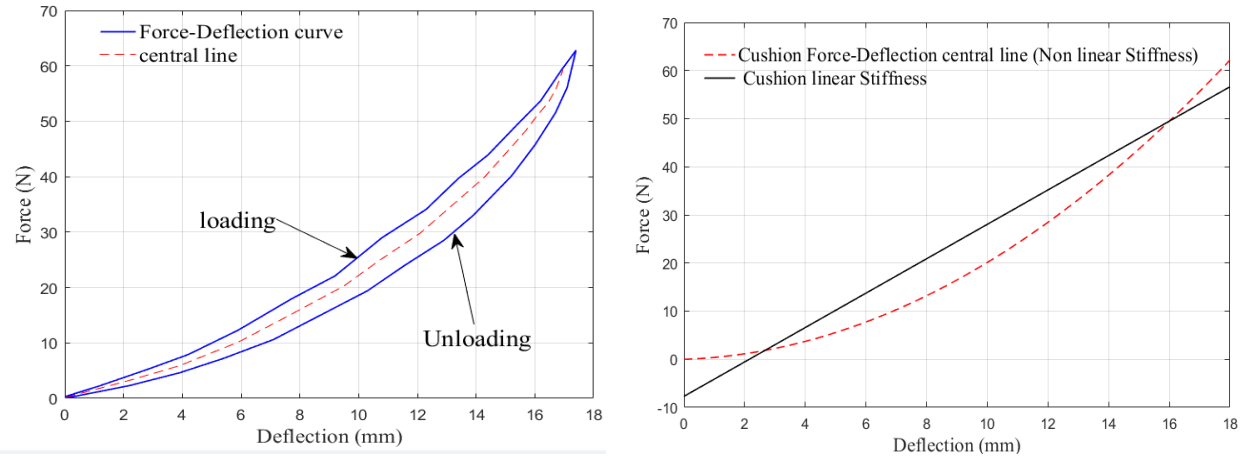

Figure 4. (a) Hysteresis loop of stiffness and central curve for polyurethane cushion (b) linear and nonlinear cushion stiffness.

As shown in Figures 4(a) and 4(b), the fitted function for the central Stiffness curve was determined. The linear function of he curve was obtained using Equation (10). The stiffness of the cushion was then analyzed through Equations (9) and (10), which describe the relationship between deformation and applied force under varying conditions.

$$F_{(K_c-\text{non linear})} = \alpha_1 z + \beta_1 z^3 \qquad (9)$$

$$F_{(K_c-\text{linear})} = \alpha_2 z + \beta_2 \qquad (10)$$

Where the $\alpha_1 = 0.21, \beta_1 = 0.25,\ \alpha_2 = 3.5$ and $\beta_2 = -7.7$

In the following sections, numerical analyses are conducted to investigate the nonlinear behavior of the spring and the damping characteristics of the cushion. Finally, the pilot comfort parameters are evaluated and compared across periodic, multi-periodic, and chaotic regions.

4. Numerical Investigation

In this section, pilot comfort is evaluated using a 5-DOF mass-spring-damper model of the seated human body coupled with a polyurethane seat cushion. The cushion's experimentally determined nonlinear stiffness is incorporated into the model, rendering the system inherently nonlinear. The resulting equations of motion (11–15) are solved numerically using the ODE45 algorithm to accurately capture the cushion's dynamic behavior.

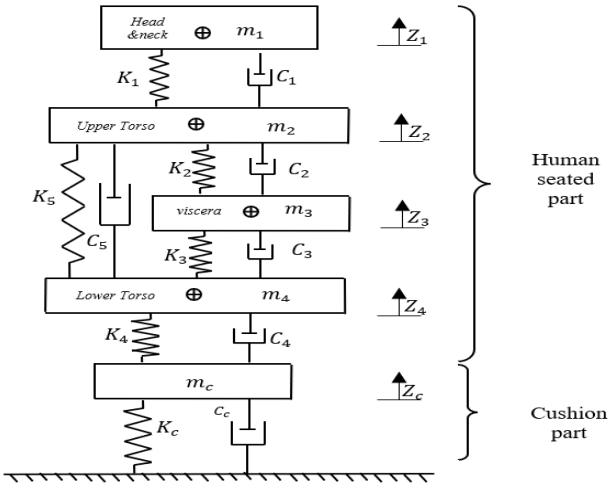

Figure 5. Seat Cushion Model with Nonlinear Stiffness

In this 5-DOF model, the total mass of the seated pilot is assumed to be 96 kg. Considering that the upper body accounts for approximately 73% of the total body mass, as reported previously [13], the mass of the pilot's upper body is estimated to be around 70 kg. The mass of each segment of the upper body, along with the corresponding spring stiffness coefficient of the interconnecting joints, are summarized in Table 2, and Equations 11 to 15 represent the formulation of this 5-DOF model.

$$m_1\ddot{z}_1 + k_1(z_1 - z_2) + c_1(\dot{z}_1 - \dot{z}_2) = 0 \quad (11)$$

$$m_2\ddot{z}_2 + c_1(\dot{z}_2 - \dot{z}_1) + k_1(z_2 - z_1) + c_2(\dot{z}_2 - \dot{z}_3) + k_2(z_2 - z_3) + c_5(\dot{z}_2 - \dot{z}_4) + k_5(z_2 - z_4) = 0 \quad (12)$$

$$m_3\ddot{z}_3 + c_2(\dot{z}_3 - \dot{z}_2) + k_2(z_3 - z_2) + c_3(\dot{z}_c - \dot{z}_4) + k_3(z_3 - z_4) = 0 \quad (13)$$

$$m_4\ddot{z}_4 + c_5(\dot{z}_4 - \dot{z}_2) + k_5(z_4 - z_2) + c_3(\dot{z}_4 - \dot{z}_3) + k_3(z_4 - z_3) + c_4(\dot{z}_4 - \dot{z}_c) + k_4(z_4 - z_c) = 0 \quad (14)$$

$$m_c\ddot{z}_c + k_4(z_c - z_4) + c_4(\dot{z}_c - \dot{z}_4) + F_{K_c} + F_{C_c} = F_0\sin(\omega t) \quad (15)$$

In equation 17, F_{K_c} , and F_{C_c} denote the stiffness and damping forces of the seat cushion, respectively. The excitation force F_0 which represents the typical loads transferred from the helicopter structure to the seat cushion. They arise primarily from rotor imbalance or aerodynamic effects. The excitation force is related to the rotor mass and the radius of gyration (r) and the angular velocity (ω^2) according to $F = mr\omega^2$ and can be expressed 80 - 120 N for the Bell 214 helicopter [31]. The excitation frequency depends on the number of rotor blades and the main rotor speed, yielding a fundamental frequency of approximately 10 Hz (ω≈62.8 rad/s). Vibrations reaching the pilot are also influenced by the tail rotor, engine, and other components, producing a spectrum of predominantly harmonic excitations. Therefore, the excitation frequency range is assumed to be 0–20 Hz. Also the 5-DOF model characteristics are shown in Table 3.

Table 3. Mass, stiffness, and damping characteristics of the seated pilot body

Parameter	Value	Parameter	Value
m_1	8.3(kg)	K_5	90 (kN/m)
m_2	30.5(kg)	C_1	400 (N.s/m)
m_3	12.7(kg)	C_2	4850 (N.s/m)
m_4	18.5(kg)	C_3	4550 (N.s/m)
m_c	0.25(kg)	C_4	2100 (N.s/m)

K_1	325(kN/m)	C_5	2100 (N.s/m)
K_2	183 (kN/m)		
K_3	162 (kN/m)		
K_4	190 (kN/m)		

$$\dot{z}_1 = v_1, \quad \dot{v}_1 = \frac{1}{m_1}\ -c_1(v_1 - v_2) - k_1(z_1 - z_2) \tag{16}$$

$$\dot{z}_2 = v_2, \quad \dot{v}_2 = \frac{1}{m_2}\ -c_1(v_2 - v_1) - c_2(v_2 - v_3) - c_5(v_2 - v_4) - k_1(z_2 - z_1) - k_2(z_2 - z_3) - k_5(z_2 - z_4) \tag{17}$$

$$\dot{z}_3 = v_3, \quad \dot{v}_3 = \frac{1}{m_3}\ -c_2(v_3 - v_2) - c_3(v_3 - v_4) - k_2(z_3 - z_2) - k_3(z_3 - z_4) \tag{18}$$

$$\dot{z}_4 = v_4, \quad \dot{v}_4 = \frac{1}{m_4}\ -c_5(v_4 - v_2) - c_3(v_4 - v_3) - c_4(v_4 - v_c) - k_5(z_4 - z_2) - k_3(z_4 - z_3) - k_4(z_4 - z_c) \tag{19}$$

$$\dot{z}_c = v_c, \quad \dot{v}_c = \frac{1}{m_c}\ -c_4(v_c - v_4) - c_c v_c - k_4(z_c - z_4) - k_c z_c + F_0 \sin(\omega t) \tag{20}$$

In this section, the state-space representation of the 5-DOF biodynamic model is used for numerical simulations, and the equations are solved using the ODE45 solver in MATLAB. This adaptive Runge-Kutta-based method, with initial conditions set to zero and the excitation frequency aligned with typical Bell 214 helicopter rotor vibrations, ensures accurate integration of the system response to harmonic excitations. The system inherently exhibits nonlinear behavior due to the nonlinear stiffness of the polyurethane cushion, making it susceptible to complex and potentially chaotic dynamics. To identify and characterize such nonlinear and chaotic behavior, bifurcation diagrams and maximum Lyapunov exponents are employed to determine the overall system response, while time histories, phase-plane trajectories, poincaré maps, and FFT-based frequency spectra are used to confirm and visualize the dynamic behaviors. In the following subsections, the nonlinear stiffness effects including cubic terms on resonant frequencies and displacement amplitudes are analyzed.

4-1 Investigation of Nonlinear Stiffness behaviors

The third-order equation governing the stiffness of the cushion, as derived from the hysteresis responses depicted in Figures 4(a) and 4(b), is presented in Equation (9). This equation incorporates the nonlinear parameter β_1, which quantifies the stiffness nonlinearity. This parameter was systematically varied and subsequently integrated into the cushion dynamics equation, as specified in Equation (17). The resulting bifurcation diagram, illustrating the system's dynamic behavior, is presented in Figure 6.

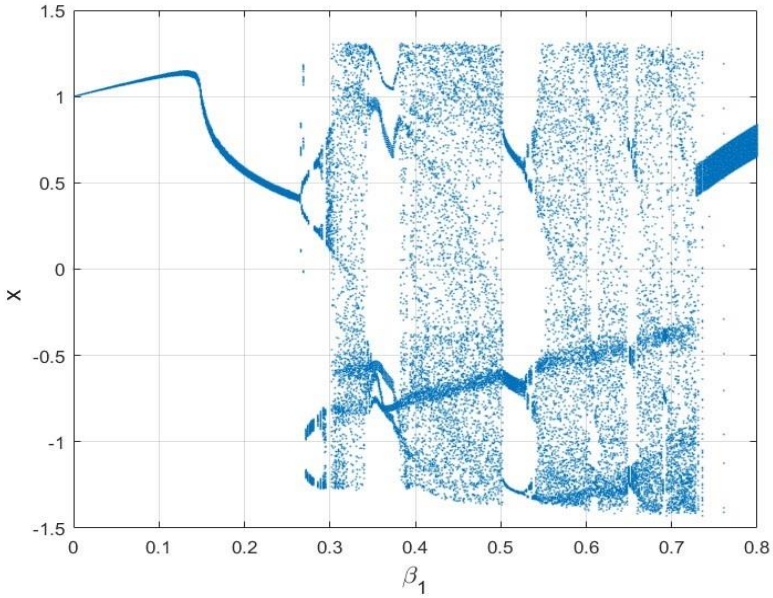

Figure 6. Bifurcation diagram with respect to the nonlinear parameter β_1

The bifurcation diagram depicted in Figure 6 provides a detailed examination of the biodynamic modeling outcomes in this study. As evident from Figure 6, at lower values of the nonlinear stiffness parameter β_1 (ranging from 0 to 0.25), the system displays stable periodic behavior, marked by regular oscillations dominated by a single frequency. As β_1 increases to the interval 0.25 to 0.28, a period-doubling bifurcation emerges, signifying the initial onset of complexity in vibration transmission from the seat and cushion through the human torso to the head. In the range β_1 = 0.29 to 0.3, the system transitions to multi-periodic motion characterized by incommensurate frequencies. Subsequently, finally, the system exits the chaotic state in the range β_1 = 0.74 to 0.8, reverting to more ordered behavior.

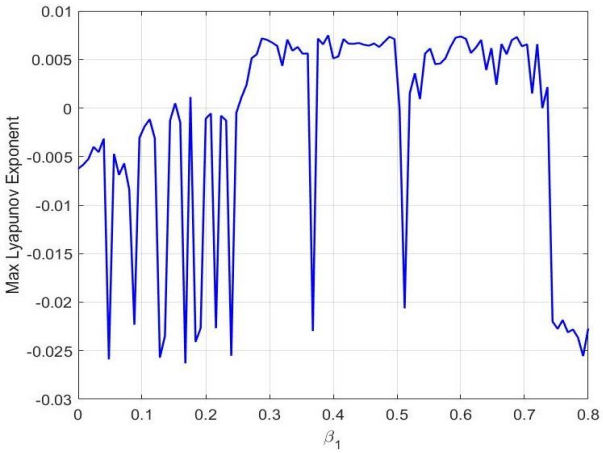

Figure 7. Maximum Lyapunov exponent of seat cushion with nonlinear stiffness parameters

In Figure. 7, the system dynamics, controlled by the control parameter β_1, are analyzed using the maximum Lyapunov exponent (MLE) spectrum, where MLE>0 indicates chaos and MLE<0 indicates stability or periodic motion. For $\beta_1 \in [0 \approx 0.28]$, the MLE is consistently negative (up to −0.025), confirming a stable region characterized by limit cycles or fixed-point absorbers. A critical transition to chaos occurs abruptly at $\beta_1 \approx 0.28$, where the MLE changes sharply to positive values. This indicates the onset of exponential divergence and the emergence of a strange attractor. This chaotic region

($\beta_1 \in [\approx 0.28, \approx 0.74]$) is interrupted by several transient stable states that appear as discrete periodic windows in which the MLE momentarily decreases to zero or less. Finally, a significant crisis is observed at $\beta_1 \approx 0.74$. Here, the system permanently exits the chaotic state as the MLE decreases sharply to very negative values, indicating a return to a very strong and stable periodic state for $\beta_1 > 0.74$. Thus, the MLE spectrum effectively depicts the complex bifurcations and transitions between the stable and chaotic dynamics inherent to the system. Specifically, Figure 7 quantitatively illustrates the system's dynamic transitions through the maximum Lyapunov exponent (MLE) spectrum, clearly identifying stable, transient, and chaotic regions. The critical transitions, periodic windows, and abrupt changes in MLE correspond well with the temporal and phase-space behaviors depicted in Figure 6. Therefore, Figure 7 serves as a complementary analytical tool that confirms and supports the qualitative observations in Figure 6, demonstrating consistency between the numerical MLE analysis and the previously observed stable and chaotic patterns.

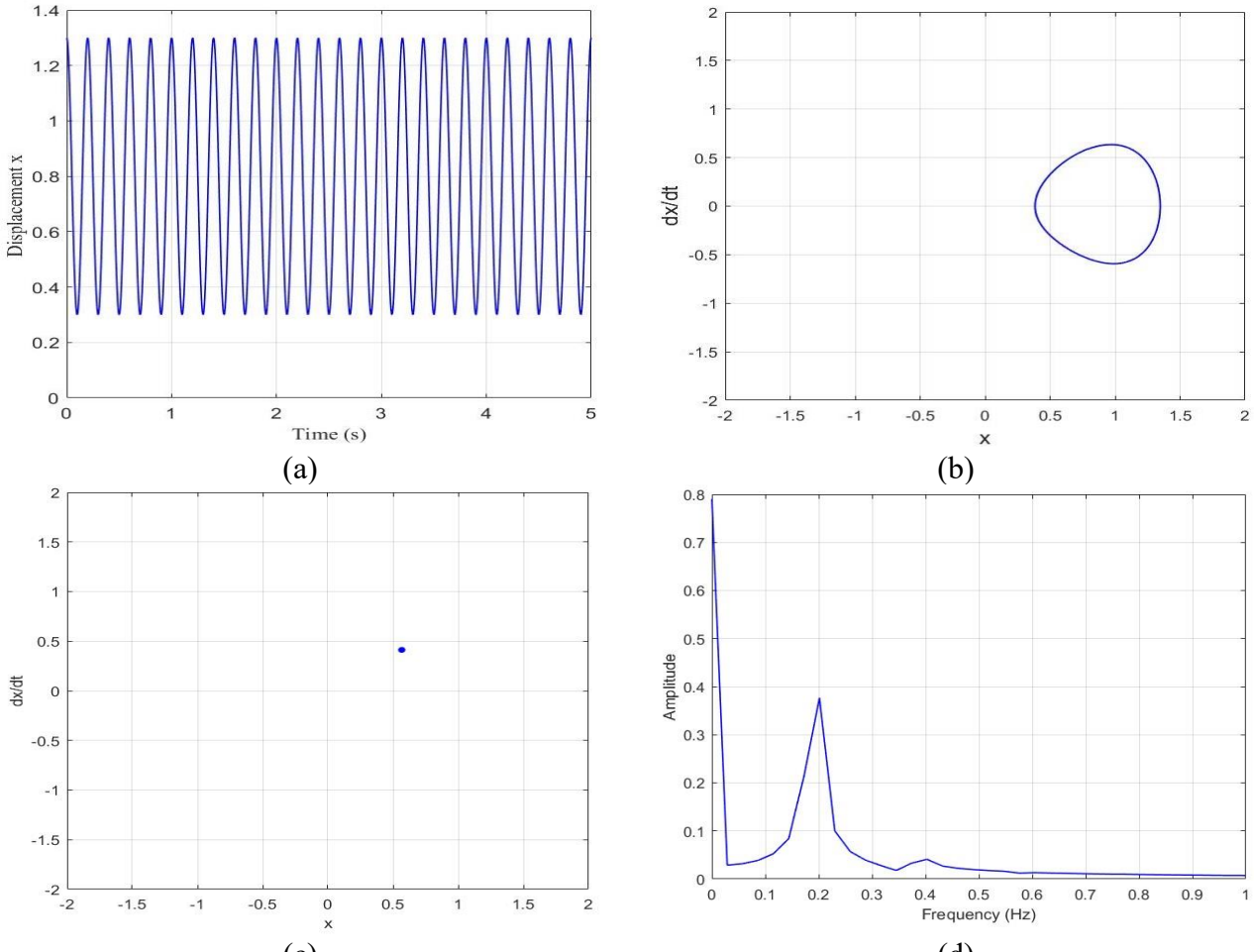

Figure 8. Dynamic responses of the nonlinear cushion model in periodic region(β_1=0.2): (a) Time response, (b) Phase plane, (c) Poincaré maps, (d) Fourier spectra

As observed in Figure 8, the cushion stiffness system operates with complete stability in the Periodic Region. This occurs at the nonlinear parameter $\beta_1 = 0.2$. This perfect, predictable behavior is crucial. It ensures optimal pilot ride comfort and low WBV. The system's stability is confirmed across all four diagnostic plots. The time response in 8(a) shows a perfectly sinusoidal and repetitive motion. The phase plane in 8(b) confirms a single, smooth closed loop. This proves the existence of a simple periodic attractor. The most definitive evidence comes from the Poincaré map in 8(c). It displays only one discrete

and concentrated point. This unequivocally confirms Period-1 motion. Finally, the Fourier Spectrum in 8(d) supports this conclusion. It shows a single, dominant, sharp peak at the excitation frequency. Virtually no energy appears at non-harmonic frequencies. The coherence across these tools verifies one key point. The stiffness system is in its most reliable and ideal operational state.

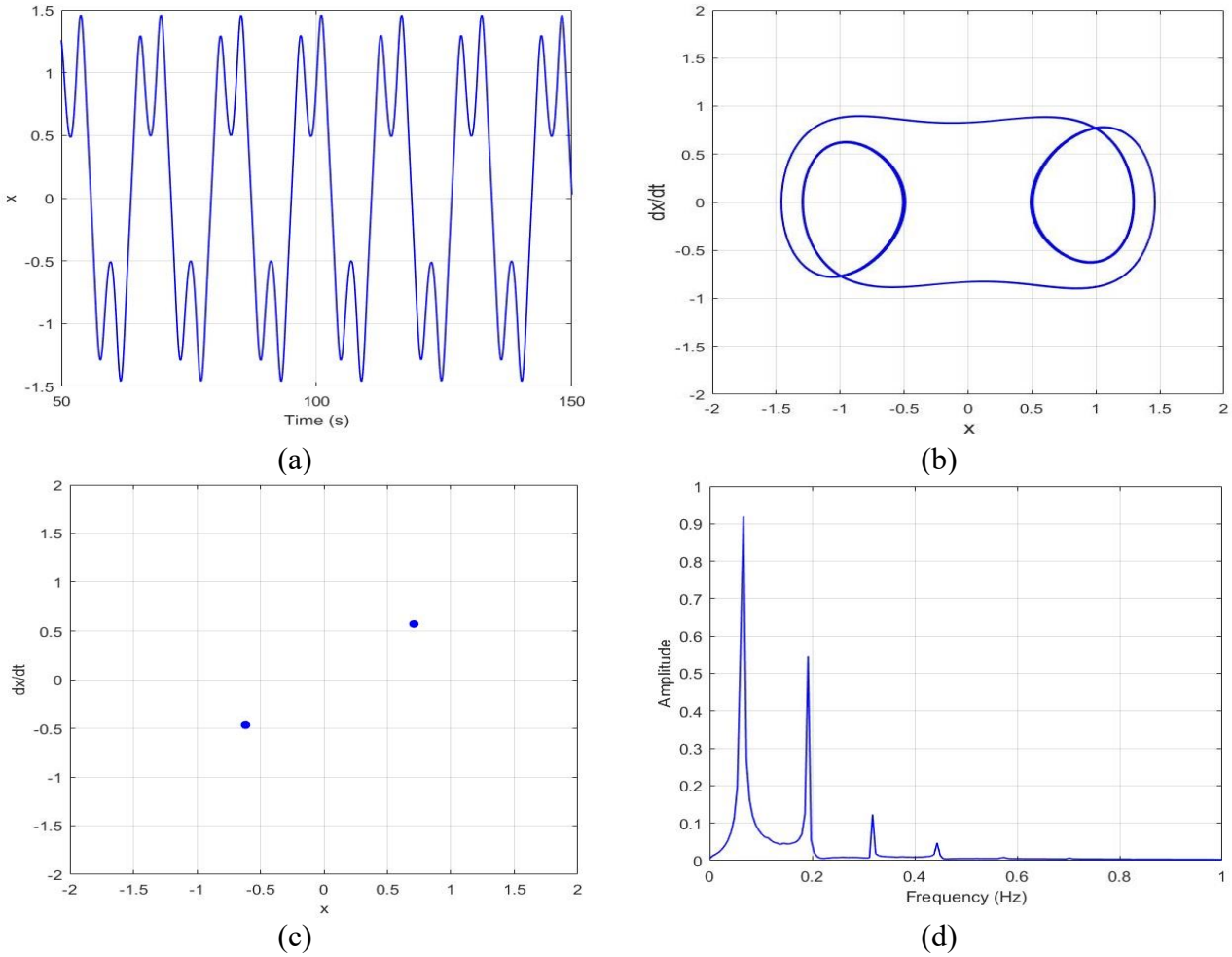

Figure 9 . Dynamic responses of the nonlinear cushion in period-doubling (β_1=0.52): (a) Time response, (b) Phase plane, (c) Poincaré maps, (d) Fourier spectra

Figure 9 comprehensively proves that the cushion stiffness system has lost its Period-1 stability and entered a period-doubling at β_1=0.52. This transition to a more complex motion, characterized by the interaction of two independent frequencies, directly results in reduced ride comfort quality and unpredictable system response.

In Figure 9(a), which shows a complex, multi-component wave, the shape is no longer a simple sinusoidal shape and indicates an irregular stiffness function. This is reflected in the phase plane of Figure 9(b), which shows a thick, dense layer absorber and a classical toroidal absorber, confirming the existence of two interacting frequencies rather than a simple period-1 loop. The poincaré plots of Figure 9(c) provide more precision and show two distinct and concentrated points. This result confirms the period-2 motion or the initial phase of the multi-periodic transition, meaning that the system repeats its state only every two excitation cycles. Finally, the Fourier spectrum of Figure 9(d) confirms this conclusion by showing two sharp, dominant peaks at incommensurate (unrelated) frequencies. The existence of these two independent frequencies is direct physical evidence of the period-2 motion of the system.

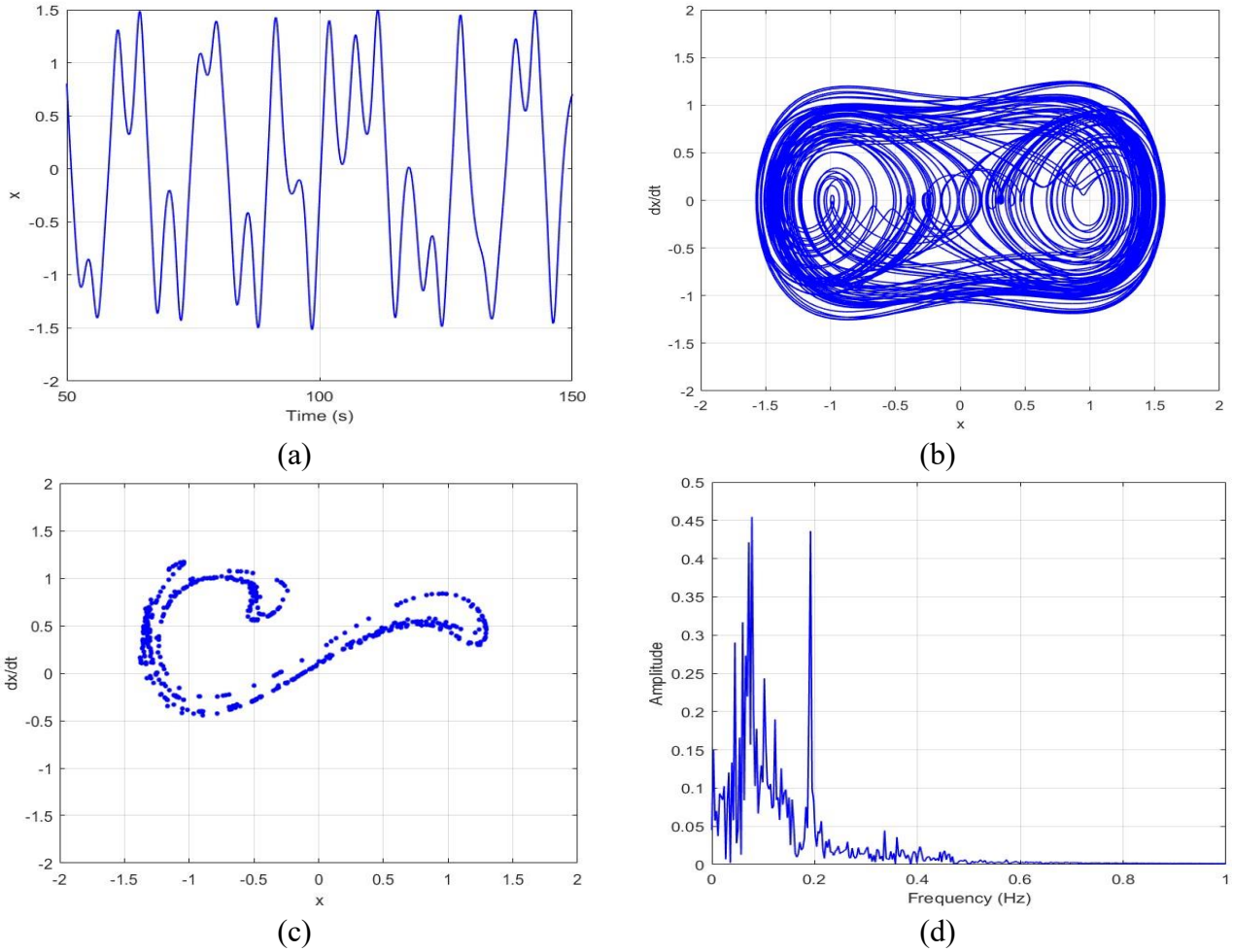

Figure 10 . Dynamic responses of the nonlinear cushion model in chaotic region (β_1=0.59): (a) Time response, (b) Phase plane, (c) Poincaré maps, (d) Fourier spectra

As shown in Figure 10, the cushion stiffness system enters a chaotic region at the nonlinear parameter β_1=0.59. This unpredictable dynamic state represents a complete loss of stiffness control.

The onset of chaos is first evidenced by the time response 10(a), which exhibits a fully irregular, non-repeating, and unpredictable waveform over time. The absence of periodicity indicates that the stiffness system operates without any recognizable pattern, exposing the pilot to entirely random vibratory forces. This irregular behavior is further illustrated in the phase Plane 10(b), which displays a strange attractor a bounded, intricate structure that occupies a region of the phase space, providing a clear signature of chaotic dynamics.

Definitive confirmation is obtained from the poincaré maps 10(c), which, rather than showing one or a few discrete points, reveal an infinite, scattered set of points forming a complex trajectory. This dispersion unequivocally validates the chaotic nature of the motion and rules out any possibility of periodic stability. Finally, the Fourier Spectra 10(d) corroborate these findings in the frequency domain, displaying a broadband spectrum with energy distributed continuously across all frequencies. This multi-frequency energy distribution explains the maximal whole-body vibration (WBV) experienced by the pilot due to the transmission of Sinusoidal vibrations.

In conclusion, the coherence of all four diagnostic tools confirms that at β_1=0.59, the stiffness system is entirely uncontrolled, severely compromising pilot safety and ride comfort as a result of unpredictable and erratic vibration transmission.

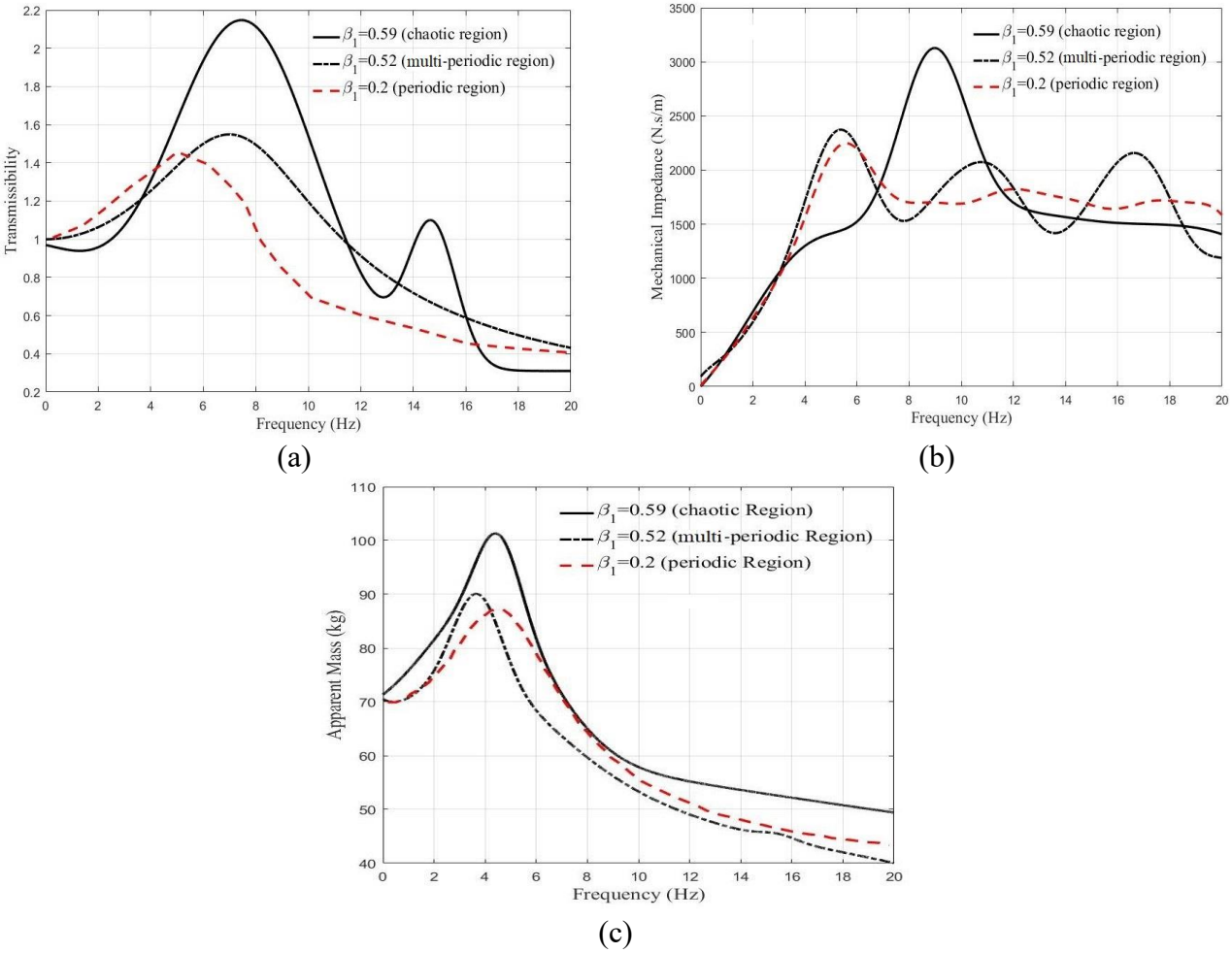

Figure 11. Comprehensive analysis of polyurethane seat cushion stiffness under periodic, multi-periodic, and chaotic region for three distinct values of the nonlinear parameter β_1,(a) transmissibility , (b) mechanical impedance and (c) apparent mass, vs frequency.

In this section, the primary objective is to maximize the ride comfort of the seated pilot and to understand how the nonlinear behavior of the polyurethane seat cushion influences pilot comfort. So far, we have identified different dynamic regions of the system, including periodic, period-doubling, and chaotic behaviors. The next step is to assess how these behaviors affect ride comfort using dedicated evaluation metrics.

Figure 11 shows a comprehensive, three-part analysis of the stiffness frequency response of the polyurethane seat cushion, controlled by the nonlinear parameter β_1, definitively proving the direct impact of each dynamic region on helicopter pilot ride comfort and Whole-Body Vibration (WBV) levels.

The Periodic region (β_1=0.2) represents the optimal performance for pilot comfort. In this state, the transmissibility 11(a) plot shows the lowest resonance peak (approx. 1.45), which effectively minimizes vibration transfer to the pilot's body, ensuring maximum ride comfort and maintaining WBV at acceptable levels. Simultaneously, both mechanical Impedance 11(b) and Apparent Mass 11(c)

responses are characterized by controlled and uniform peaks, indicative of an effective and predictable isolation system.

As nonlinearity increases, the system transitions into the period-doubling (β_1=0.52), a detrimental state where resonance peaks increase across all three metrics and plots become more irregular. This transition results in a perceptible decrease in pilot comfort due to uneven vibration exposure, which increases fatigue and may reduce operational accuracy.

Crucially, the system reaches its worst dynamic state in the chaotic region (β_1=0.59). Here, transmissibility 11(a) reaches its highest peak (over 2.15), signifying maximum transfer of harmful vibrations to the pilot, leading directly to a severe increase in WBV, acute discomfort, and heightened risk of long-term physical damage. This degradation is corroborated by the mechanical impedance 11(b) plot, which exhibits the highest and sharpest resistance peaks (over 3000 N.s/m), confirming that the nonlinear stiffness actively generates the largest reactive forces in response to excitation. Likewise, the Apparent Mass (c) shows its maximum peak (approx. 100 kg), indicating maximum generation of inertial forces.

5. Conclusion

This study successfully investigated the existing gap in understanding the nonlinear and potentially chaotic dynamics of polyurethane seat cushions, particularly their impact on Bell 214 helicopter pilot comfort. By integrating experimental determination of cushion parameters nonlinear stiffness with a 5-DOF biodynamic pilot model, we provided a comprehensive framework for assessing vibration isolation under complex excitations.

The numerical and experimental investigation demonstrated a critical dependence on the nonlinear parameters:

- The dynamic characteristics of the polyurethane seat cushion were first obtained experimentally, revealing pronounced nonlinear behavior in the cushion stiffness. These measurements provided a fundamental basis for subsequent numerical analyses and for understanding how the cushion's nonlinear properties influence pilot ride comfort under various dynamic conditions.
- Using appropriate analytical and numerical tools, the various dynamic behaviors of the system, including periodic, period-doubled (multi-periodic), and chaotic regions, were accurately identified. This step provided a solid foundation for understanding how each type of system behavior affects the pilot's ride comfort.
- Increasing the nonlinear stiffness parameter β_1 drives the system from an optimal periodic region (β_1 = 0.2), with controlled transmissibility (~1.45) and predictable mechanical impedance and apparent mass peaks, to a chaotic region (β_1 = 0.59). In this chaotic state, the transmissibility increases from 2.15, mechanical impedance peaks exceeding 3000 N.s/m and apparent mass to about 100 kg, indicating maximum vibration transmission and severe WBV. This indicates that the periodic region is functionally superior for maintaining pilot comfort, while crossing the critical threshold β_1 turns the cushion into an uncontrolled vibration amplifier.
- The results indicate that nonlinear stiffness (β_1) critically influence vibration transmission and pilot comfort. To maintain the system within the optimal periodic region designers should avoid values of β1 that lead to chaos.

For future studies it is recommended that future studies focus on modifying the seat cushion's material composition so that its nonlinear stiffness and damping properties prevent transition into multi period or

chaotic behaviors. By ensuring vibrations remain within the periodic region, predictable isolation is achieved, maximizing ride comfort and minimizing Whole-Body Vibration (WBV) exposure.

Funding Declaration
This research did not receive any specific grant from funding agencies in the public, commercial, or not-for-profit sectors.

Competing Interests
The authors declare no competing financial or non-financial interests

References

[1] R. Saengwong-ngam, H. Kitazawa, Cushion performance of eco-friendly natural rubber latex foam composite with bamboo leaf fiber for impact protection of guava, Postharvest Biol Technol 208, 2023, http://dx.doi.org/10.1016/j.postharvbio.2023.112663.

[2] S. Zhu, R. Dong, Z. Lu, Y. Guo, Z. Liu, H. Liu, A finite element method study of the effect of vibration on the dynamic biomechanical response of the lumbar spine, Clinical Biomechanics, 2023, https://doi.org/10.1016/j.clinbiomech.2023.106164

[3] W. Yin, J. Ding, Y. Qiu, Nonlinear Dynamic Modelling of a Suspension Seat for Predicting the Vertical Seat Transmissibility 2021, http://dx.doi.org/10.1155/2021/3026108.

[4] P. Mondal, S. Arunachalam, Finite Element Modelling of Car Seat with Hyperelastic and Viscoelastic Foam Material Properties to Assess Vertical Vibration in Terms of Acceleration, Engineering 12, 2020, https://doi.org/10.4236/eng.2020.123015.

[5] Gobbi, Massimiliano, et al. "A local approximation based multi-objective optimization algorithm with applications." *Optimization and Engineering* 15.3 2014. https://doi.org/10.1007/s11081-012-9211-5.

[6] YANG, Judy P.; FENG, Ting-Yu. Enhancing a three-mass vehicle model with wheel-size effect for scanning bridge frequencies. International Journal of Applied Mechanics, 2023,. https://doi.org/10.1142/S1758825123500564.

[7] V. A. Atindana et al., “Experimental design and optimization of pneumatic low-frequency driver seat for off-road vehicles: quasi-zero negative stiffness and gray wolf optimization algorithm,” Journal of the Brazilian Society of Mechanical Sciences and Engineering, vol. 45, no. 9, p. 502, 2023. https://doi.org/10.1007/s40430-023-04391-8

[8] Marzban Rod J, A review study of the vibrations caused to the human sitting and providing an optimal biomechanical model of the car occupant using genetic algorithm, 2016, http://dx.doi.org/10.1007/s42417-018-0054-z.

[9] Khavanin A, Health risk assessment due to exposure to whole body vibration using ISO 2631-1 and BS 6841 standards, 2013, https://doi.org/10.7508/jrh.2016.04.002.

[10] T.E. Fairley, M.J. Griffin, The Apparent Mass of the Seated Vertical Vibration Human Body, 1989, https://doi.org/10.1016/0021-9290(89)90031-6.

[11] C. Corbridge, M.J. Grifftn, Vibration and comfort: Vertical and lateral motion in the range 0·5 to 5·0 Hz, Ergonomics 29,1986, https://doi.org/10.1080/00140138608968263.

[12] P.-E. Boileau, S. Rakheja, Whole-body vertical biodynamic response characteristics of the seated vehicle driver Measurement and model development, 1998, https://doi.org/10.1016/S0169-8141(97)00030-9.

[13] Y. Chen, V. Wickramasinghe, D. Zimcik, Development and evaluation of hybrid seat cushions for helicopter aircrew vibration mitigation, in: J Intell Mater Syst Struct, SAGE Publications Ltd, 2015: pp. 1633–1645. https://doi.org/10.1177/1045389X14566522.

[14] P.E. Boileau, A Study of Secondary Suspensions and Human Driver Response to Whole-Body Vehicular Vibration and Shock, 1995, https://api.semanticscholar.org/CorpusID:107673735.

[15] M.J. Griffin, Measurement, evaluation, and assessment of occupational exposures to hand-transmitted vibration, 1997, https://doi.org/10.1136/oem.54.2.73.

[16] S.A. Pankoke S., Latest development in occupant simulation techniques related to seating comfort and human response and human response to vibration: finite element occupant model CASIMIR, United Kingdom Conference on Human Responses to Vibration 2008, DOI:10.4271/2007-01-2459.

[17] A.M.A. Soliman, Measurement and modelling of the y-direction apparent mass of sitting human body-cushioned seat system, J Sound Vib 322,2009, http://dx.doi.org/10.1016/j.jsv.2008.11.002.

[18] G.J. Stein, P. Múčka, R. Chmúrny, B. Hinz, R. Blüthner, Measurement and modelling of x-direction apparent mass of the seated human body-cushioned seat system, J Biomech 40 2007, http://dx.doi.org/10.1016/j.jsv.2008.11.002.

[19] C. Zhang, Y. Zhao, Y. Shen, and D. Li, “The modeling and analysis of vibration response with airdrop vehicle in landing process,” Journal of the Brazilian Society of Mechanical Sciences and Engineering, vol. 46, no. 6, p. 345, 2024. https://doi.org/10.1007/s40430-024-04913-y.

[20] C. Xu et al., “Vibration analysis and control of semi-active suspension system based on continuous damping control shock absorber,” Journal of the Brazilian Society of Mechanical Sciences and Engineering, vol. 45, no. 6, p. 341, 2023. https://doi.org/10.1007/s40430-023-04183-0

[21] Mo, S., Wang, Z., Zeng, Y., & Zhang, W, Nonlinear vibration analysis of the coupled gear-rotor-bearing transmission system for a new energy vehicle. International Journal of Bifurcation and Chaos, 33(09), 2350105, 2023. https://doi.org/10.1142/S0218127423501055.

[22] Pan, W., Ling, L., Qu, H., & Wang, M. Nonlinear vibration of bolted rotor bearing system accounting for the bending stiffness characteristics of the connection interface. International Journal of Bifurcation and Chaos, 33(04), 2350050. 2023. https://doi.org/10.1142/S0218127423500505.

[23] Bhatia, Akash, et al. "Comparative study of different seat cushion materials to improve the comfort of tractor seat." Journal of The Institution of Engineers (India): Series A 103.2, 387-396, 2022. https://doi.org/10.1007/s40030-022-00622-8.

[24] Fakhraei, J., Khanlo, H. M., Ghayour, M., & Faramarzi, K. The influence of road bumps characteristics on the chaotic vibration of a nonlinear full-vehicle model with driver. International Journal of Bifurcation and Chaos, 26(09), 1650151, 2016, https://doi.org/10.1142/S0218127416501510.

[25] Dehghani, R., H. M. Khanlo, and J. Fakhraei. "Active chaos control of a heavy articulated vehicle equipped with magnetorheological dampers." *Nonlinear Dynamics* 87.3 ,1923-1942, 2017. https://doi.org/10.1007/s11071-016-3163-9.

[26] Fakhraei, J., Khanlo, H. M., & Dehghani, R. Nonlinear dynamic behavior of a heavy articulated vehicle with magnetorheological dampers. Journal of Computational and Nonlinear Dynamics, 12(4), 041017. 2017, https://doi.org/10.1115/1.4035669.

[27] Zhao, Leilei, et al. "Analytical simulation of dynamic characteristics of seat system with nonlinear suspension considering friction effects." International Journal of Modeling, Simulation, and Scientific Computing 11.06, 2050058. 2020. https://doi.org/10.1142/S1793962320500580.

[28] P. Magri, M. Gadola, D. Chindamo, and G. Sandrini, "A comprehensive method for computing non-linear elastokinematic properties of passenger car suspension systems: Double wishbone case study," *Journal of Computational and Nonlinear Dynamics*, vol. 19, no. 10, p. 101006, Oct. 2024. https://doi.org/10.1115/1.4066092.

[29] Chunyan, K., Guangli, L., Yongxi, L., Mingkun, Y., Yi, L., Jie, X., Yi, W., and Guomin, L. (July 14, 2025). "Multifactor Analysis of Static and Dynamic Characteristics of Membrane Air Springs for Small Passenger Cars." ASME. J. Comput. Nonlinear Dynam. October, 2025 20(10): 101005. https://doi.org/10.1115/1.4068976

[30] Zhao, H., Fu, C., Zhu, W. et al. Dynamic characteristics and sensitivity analysis of a nonlinear vehicle suspension system with stochastic uncertainties. Nonlinear Dyn 112, 21605–21626, 2024. https://doi.org/10.1007/s11071-024-10159-z

[31] Kamali, Seyed Mohammad, et al. "Investigating The Effect of Seat Suspension System and Cushion on The Dynamic Behavior of the 214 Helicopter Pilot's Body." AUT Journal of Mechanical Engineering 9.4, 431-446. 2025. https://dx.doi.org/10.22060/ajme.2025.23838.6161.